A&A manuscript no.
(will be inserted by hand later)

Your thesaurus codes are:
6(02.01.2; 11.01.2; 11.05.1; 11.09.1 (NGC 1052); 11.14.1; 13.25.2)

ASTRONOMY AND ASTROPHYSICS

On the hypothesis of an advection-dominated flow in the core of NGC 1052: new constraints from a BeppoSAX observation

M. Guainazzi[1], **T. Oosterbroek**[2], **L.A. Antonelli**[3], **G. Matt**[4]

[1] XMM-Newton SOC, VILSPA, ESA, Apartado 50727, 28080 Madrid, Spain
[2] Astrophysics Division, Space Science Department of ESA, ESTEC, Postbus 299, NL-2200 AG Noordwijk, The Netherlands
[3] Osservatorio Astronomico di Roma, Via dell'Osservatorio, I-00044 Monteporzio Catone, Italy
[4] Dipartimento di Fisica, Università degli Studi Roma Tre, Via della Vasca Navale 84, I-00046 Roma, Italy

Received ; accepted

Abstract. We report the results of a broadband (0.1–100 keV) X-ray observation of the nearby elliptical galaxy NGC 1052, performed with the BeppoSAX observatory. We confirm the presence of a bright (2–10 keV luminosity $\sim 4 \times 10^{42}$ erg s^{-1}) and strongly absorbed ($N_{\rm H} \sim 2 \times 10^{23}$ cm^{-2}) X-ray source. The flatness of the X-ray spectrum (photon index, Γ, $\simeq 1.4$), the estimated low accretion rate ($\dot{m} \equiv \dot{M}/\dot{M}_{\rm Edd} \sim 10^{-4}$) and the radio-to-X-ray spectral energy distribution suggest that this observation may represent the first direct measurement above 10 keV of an accretion-dominated flow in an elliptical galaxy.

Key words: Accretion – Galaxies:active – Galaxies:elliptical and lenticular – Galaxies:individual:NGC 1052 – Galaxies:nuclei – X-ray:galaxies

1. Introduction

The discovery of supermassive black holes (10^6–$10^9 M_\odot$) in the nuclei of several nearby galaxies (Magorrian et al. 1998) has raised the question of why most of them are not active. A possible solution is provided by the so called Advection Dominated Accretion Flows (ADAF; Rees 1982; Narayan & Yi 1995; Fabian & Rees 1995). In this class of accretion solutions, the accreting gas is so tenuous that it cannot cool efficiently, the viscous energy is stored in the protons as thermal energy and eventually advected onto the nuclear compact object. The ADAFs are therefore characterized by small radiative efficiency and accretion rates ($\dot{m} \equiv \dot{M}/\dot{M}_{\rm Edd} < 10^{-1.6}$; Narayan & Yi 1995; Rees et al. 1982). At low $\dot{m}$ the hard X-ray emission is mainly due to bremsstrahlung emission from a population of $\sim$100 keV electrons, and is therefore much harder than typically observed in Seyfert galaxies (Nandra et al. 1997; Turner et al. 1997; Matt 2000).

Recently, hard X-ray tails have been discovered in the ASCA spectra of several elliptical galaxies (Allen et al 2000). Photon indices are in the range 0.6–1.5, therefore remarkably consistent with the expectations of the ADAF scenario. Unfortunately, the ASCA energy bandpass is limited to 9–10 keV, and the detection of these hard tails is therefore difficult and somewhat model-dependent.

One of the most intriguing of these ADAF-candidates is the nearby ($z = 0.0049$) elliptical galaxy NGC 1052. It is a narrow-line LINER (Heckman 1980), with a compact radio core (diameter $\simeq 0.14$ pc) and a radio halo of about 3 kpc diameter. NGC 1052 is the first type 2 LINER where broad lines in spectropolarimetric measurements have been discovered (Barth et al. 1999). The ASCA spectrum (Guainazzi & Antonelli 1999, G99; Weaver et al. 1999) is extremely flat: a formal fit with a simple power law yields a photon index $\Gamma \simeq 0.1$. This suggests either high photoelectric absorption (column density $N_{\rm H} \simeq 10^{23}$ cm^{-2}) or a Compton-reflection dominated spectrum (which, of course, would imply an even more strongly absorbed active nucleus). In the former scenario the intrinsic spectral index is still very flat ($\Gamma \simeq 1.2$). This is intriguingly consistent with the ADAF scenario.

The ASCA results prompted a BeppoSAX program of observations of narrow-line LINERs with broad spectropolarimetric lines, mainly focused to investigate their hard X-ray spectrum ($\gtrsim$10 keV). The results of this experiment on NGC 1052 are reported in this paper.

2. Observation and data reduction

BeppoSAX observed NGC 1052 between 2000 January 11 (19:27 UT) and 13 (08:57 UT). The instruments were operating in nominal direct modes. Data reduction and analysis followed standard procedures, as detailed, *e.g.*, in Guainazzi et al. (1999). Scientific products from the imaging instruments (Low Energy Concentrator Spectrometer, LECS; Parmar et al. 1997; Medium Energy Concentrator Spectrometer, MECS; Boella et al. 1997) were extracted from circular regions around the galaxy X-ray centroid of radii 2′ and 4′, respectively. Background subtraction was performed using deep blank sky field exposures, accumulated by the BeppoSAX Science Data Center (SDC). The background-subtracted net count rates are $(1.26 \pm 0.09) \times 10^{-2}$ s^{-1} and $(3.71 \pm 0.08) \times 10^{-2}$ s^{-1}, in the LECS (0.1–4 keV) and MECS (1.8–10.5 keV), respectively, corresponding to exposure times of 25.8 and 63.2 ks.

Send offprint requests to: M.Guainazzi

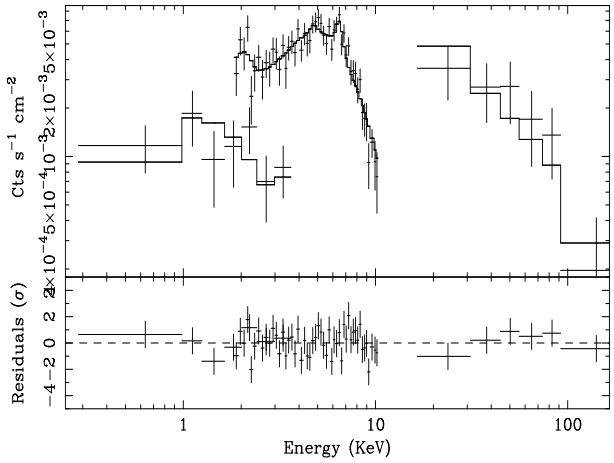

Fig. 1. Spectrum plus best-fit model (*upper panel*) and residuals in units of standard deviations (*lower panel*) when the model "P" is applied to the broadband BeppoSAX NGC 1052 spectrum

Spectral analysis made use of the latest response matrices released by the SDC in January 2000.

In what follows: energies are quoted in the source rest frame, and errors are at 90% confidence level for one interesting parameter ($\Delta\chi^2 = 2.71$), unless otherwise specified.

3. Results

3.1. The PDS spectrum ($E > 10$ keV)

The 60.0 ks exposure time on NGC 1052 allowed a PDS detection, with a total 13–200 keV count rate of 0.22 ± 0.04 s^{-1}. If we take into account the typical systematic uncertainties associated with the PDS background subtraction algorithm (Guainazzi & Matteuzzi 1997), the detection is at a level higher then 5σ in the 13–90 keV band (see Fig. 1). No known hard X-ray bright source is present in the $(1.3^\circ)^2$ PDS field of view. The number of expected sources with flux equal or higher than NGC 1052 is $\lesssim 0.06$ according to the Cagnoni et al. (1998) logN-logS relation. A simple power-law fit of the PDS spectrum yields a very flat index: $\Gamma = 1.0\pm^{0.7}_{0.3}$.

3.2. The broadband BeppoSAX Spectrum (0.1–100 keV)

The source did not show any significant X-ray variability during the BeppoSAX observation. The reduced χ^2, when a constant line is fit to the $\Delta t = 5760$ s light curve are $\chi^2_\nu = 0.76$ and $\chi^2_\nu = 0.78$ in the 0.1–2 keV (LECS) and 2–10 keV (MECS) energy bands, respectively. We will therefore focus in this Section on the time-averaged spectra only.

A photoelectrically-absorbed single component model provides an inadequate fit of the broadband (0.1–100 keV) BeppoSAX spectrum (*e.g.*: $\chi^2 = 185.4/80$ degrees of freedom, dof, if a power-law model is employed). On the other hand, a very good fit ($\chi^2_\nu \simeq 1.02$–1.03) is obtained with a two-component model, constituted by an absorbed ($N_{\rm H} \simeq$ a few 10^{23} cm^{-2}) power-law plus a "soft excess" below 2 keV. The limited statistics prevents us from unambiguously characterizing the latter component. In the following we will discuss, as illustrative examples, models where this soft excess is described: either with a power-law ("P" model hereinafter), whose index is held fixed to that of the high-energy absorbed power-law (thus modeling reflection of the nuclear continuum, scattered by an electron plasma - "warm mirror" - along our line of sight; Antonucci & Miller 1985); or with thermal emission from a collisionally ionized, optically thin plasma (`mekal` model in XSPEC; "M" model hereinafter). Model "P" also describes a geometry, in which the absorber only covers a fraction of the line of sight. The best-fit parameters are reported in the upper panel of Tab. 1. As already suggested by the analysis of the PDS spectrum alone, the absorbed power-law component is rather flat ($\Gamma \simeq 1.4$). If the power-law in model "P" is substituted by a thermal bremsstrahlung ($\chi^2 = 83.6/77$ dof), its temperature is $150\pm^{720}_{100}$ keV.

The addition of a narrow Gaussian emission line is required at the 98.9% confidence level, according to the F-test, in the "P" model ($\Delta\chi^2|_P = 10$ for a decrease of the degrees of freedom by two), whereas only at the 90.9% level in the "M" model ($\Delta\chi^2|_M = 5$). The Gaussian line centroid energy is consistent, within the statistical uncertainties, with K_α fluorescent emission from neutral iron. However, the EW of the iron line system is too large to be produced in transmission by the same cold matter, which is responsible for the attenuation of the X-ray continuum (which would imply $EW \simeq$130 eV for a spherical distribution of matter; Leahy & Creighton 1993). No iron emission line is expected from an ADAF. The slight difference in EW between models "P" and "M" (in the latter the iron line profile is partly accounted by the emission of the thermal plasma) may suggest a multi-component structure of the iron line, which is unresolved by the MECS. Ionized iron lines could be also produced by the "warm mirror" (Netzer & Turner 1997). We have therefore repeated the fit in the "P" scenario, assuming that the iron emission actually consists of two components: one neutral ($E_{\rm c} = 6.4$ keV) and one He-like ($E_{\rm c} = 6.7$ keV). The fit is of comparable quality ($\chi^2 = 79.8/77$ dof), with: EW(6.4 keV) $= 170\pm^{170}_{150}$ eV; EW(6.7 keV) $= 180\pm^{150}_{160}$ eV. The soft excess continuum flux at 6 keV is about 1/3 of that of the transmitted component. Therefore, the EW of the ionized iron line against its proper continuum would be of the correct order of magnitude if produced in a "warm mirror" (Matt et al. 1996). The neutral component EW is now consistent with being produced in transmission by the same matter covering the active nucleus, if its covering factor is large.

A hard X-ray continuum could be in principle due to Compton reprocessing of the nuclear continuum, by either the accretion disc (George & Fabian 1991; Matt et al. 1992) or the molecular torus encompassing the active nucleus (Ghisellini et al. 1994; Krolik et al. 1994). This scenario does not, however, match our data. A fit, where the absorbed high-energy component is a bare face-on Compton-reflection (model `pexriv` in XSPEC; Magdziarz & Zdziarski 1995) is statistically unac-

Model	$N_{\rm H}$ 10^{23} cm^{-2}	Γ	$kT/f_{\rm s}$ (keV/%)	$E_{\rm c}$ (keV)	EW (eV)	χ^2/dof
BeppoSAX						
M	$2.0\pm^{0.6}_{0.5}$	$1.39\pm^{0.25}_{0.18}$	>5	$6.48\pm^{0.16}_{0.20}$	230 ± 170	77.7/76
P	2.1 ± 0.5	$1.45\pm^{0.20}_{0.16}$	$20\pm^{15}_{11}$	$6.54\pm^{0.17}_{0.14}$	310 ± 70	79.6/77
ASCA-ROSAT						
M	$0.9\pm^{0.6}_{0.3}$	$1.0\pm^{0.5}_{0.4}$	>9	$6.35\pm^{0.07}_{0.06}$	220 ± 110	296.0/309
P	1.2 ± 0.2	1.22 ± 0.16	$26\pm^{15}_{9}$	6.36 ± 0.06	300 ± 110	297.0/310
ASCA-BeppoSAX-ROSAT						
M	$2.0\pm^{0.6}_{0.5}{}^{a}$ $1.2\pm^{0.3}_{0.2}{}^{b}$	1.4 ± 0.2	>11	$6.38\pm^{0.07}_{0.06}$	280 ± 90	383.0/444
P	1.9 ± 0.4^{a} $1.18\pm^{0.18}_{0.16}{}^{b}$	$1.33\pm^{0.09}_{0.08}$	$22\pm^{4}_{5}$	$6.40\pm^{0.06}_{0.07}$	300 ± 90	386.0/445

Table 1. Best-fit parameters and results when the models "M" and "P" (details in text) are applied to the NGC 1052 broadband spectrum of BeppoSAX (*upper panel*), ASCA-ROSAT (after G99; *central panel*), and ASCA-BeppoSAX-ROSAT (*lower panel*). $f_{\rm s}$ is the scattering fraction (defined as the 2–10 keV flux ratio between the transmitted and the scattered power-law components). $E_{\rm c}$ and EW are the centroid energy and the equivalent width of the emission line, respectively.

[a] BeppoSAX
[b] ASCA

ceptable ($\chi^2 = 112.6/76$ dof). The addition of a Compton-reflection component to the "P" model (where only the relative normalization between the reflected and the direct component, R, and the intrinsic power-law cut-off energy are left free parameters in the fit; an inclination angle of 30° and solar abundances are assumed) does not significantly improve the fit ($\chi^2 = 79.1/75$ dof). The 90% upper limit for two interesting parameter on R is 0.6 (for $\Gamma < 1.65$). These results allow us to rule out one class of models, which adequately fit the ASCA-ROSAT spectra, hence favoring the G99 transmission scenario.

The observed flux in the 0.5–2 keV (2–10 keV) energy band is 0.4 (4.0)$\times10^{-12}$ erg cm^{-2} s^{-1}. This corresponds to a luminosity of 0.4 (4.2)$\times10^{41}$ erg s^{-1}.

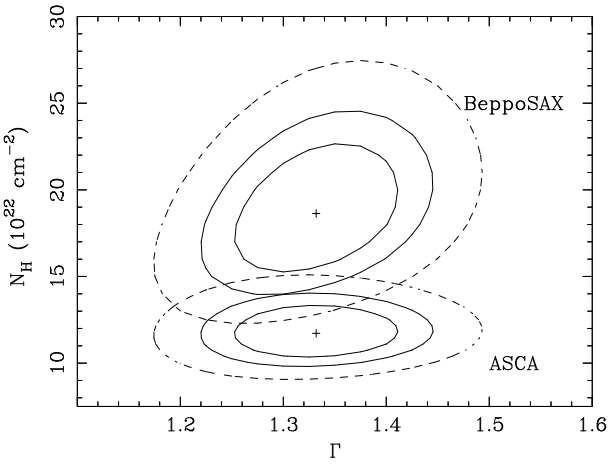

Fig. 2. Spectral index versus column density iso-χ^2 contour plots, when the ""P" model is simultaneously applied to the ASCA, BeppoSAX and ROSAT spectra. The column density is left free to vary independently in the BeppoSAX and ASCA/ROSAT models (*labels*). The contours correspond to the 68%, 90% (*solid lines*) and 99% (*dashed line*) confidence levels for two interesting parameters.

3.3. Comparison with ROSAT and ASCA data

In the central panel of Tab. 1, the best-fit parameters are reported, when the "M" and "P" models are applied to the ASCA and ROSAT spectra of NGC1052 (see the Tab. 1 in G99). NGC 1052 was comparatively bright during the August 1996 ASCA (2–10 keV flux $\simeq3.5\times10^{-11}$ erg cm^{-2} s^{-1}) and the January 2000 BeppoSAX observations. The only spectral parameter showing a significant difference is the absorbing column density, which was about a factor of 2 higher in the later BeppoSAX observation. The spectral indices measured by BeppoSAX tend also to be slightly softer, but still consistent with the ASCA-ROSAT measurements within the statistical uncertainties.

We have performed a simultaneous fit of the ROSAT, ASCA and BeppoSAX spectra, to check whether the improved statistics allows us to distinguish between the "M" and "P" models. In these fits only the column density absorbing the primary nuclear continuum has been allowed to vary independently in the BeppoSAX and ASCA-ROSAT models (ROSAT spectra are basically insensitive to column densities of the order of 10^{23} cm^{-2}). Normalization constants have been included as free parameters in the models, to account for the different fluxes measured in the three observations. The results are reported in the lower panel of Tab. 1. The two models yield comparably good fits ($\chi^2|_P = 386.0/445$ dof; $\chi^2|_M = 383.0/444$ dof). Better data quality is needed to resolve this issue. The spectral index is indeed much better constrained than by BeppoSAX data alone, and still very flat (see Fig. 2).

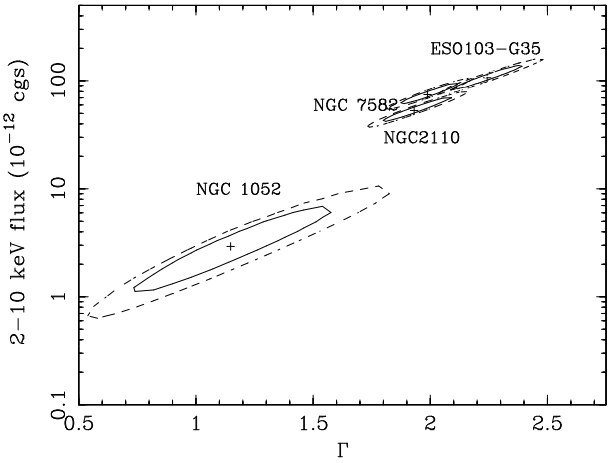

Fig. 3. Spectral index versus extrapolated 2–10 keV flux iso-χ^2 contours if a simple power-law model is applied to the PDS spectrum of NGC 1052 and of the "flat" Seyfert 2s of Turner et al. (1997). The levels are 68% (*solid line*) and 90% (*dashed line*) for two interesting parameters

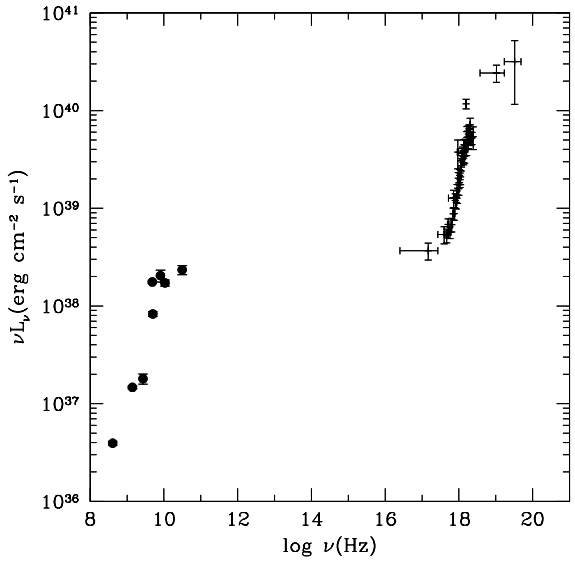

Fig. 4. Radio-to-X-ray SED of NGC 1052

4. Discussion

NGC 1052 is the first "type 2" LINER, where broad lines were discovered in spectropolarimetric measurement (Barth et al. 1999). One may therefore expect that its X-ray spectrum resembles that of Seyfert 2 galaxies, where the luminous nuclear emission is photoelectrically absorbed by matter with a substantial column density. The observation performed with BeppoSAX demonstrates that this is indeed the case, thanks to the first measure of the broadband (0.1–100 keV) X-ray spectrum of this object.

Even more intriguing is the nature of the accretion flow in this AGN. The nuclear spectrum is rather flat ($\Gamma \simeq 1.4$), as the ASCA observation had already suggested (G99; Weaver et al. 1999). The best-fit value is inconsistent at 2σ level with the distribution of spectral indices observed in Seyfert 1s ($\langle\Gamma_{\rm Sy1}\rangle = 1.87$; $\sigma_{\rm Sy1} = 0.22$; Nandra et al. 1997; Reynolds 1997) and radio-quiet quasars ($\langle\Gamma_{\rm RQQ}\rangle = 1.93$; $\sigma_{\rm RQQ} = 0.22$; Reeves & Turner 2000). It is closer to the distribution of spectral indices in radio-loud quasars ($\langle\Gamma_{\rm RLQ}\rangle = 1.6$; $\sigma_{\rm RLQ} = 0.15$; Reeves & Turner 2000). However, NGC 1052 radio-loudness, according to the Wilkes & Elvis (1987) definition, is 1.1, therefore pointing to a radio-quiet or, at most, a borderline object. There are some Seyfert 2s, whose ASCA spectral indices (Turner et al. 1997) are as flat as those measured in NGC 1052. Recently, Malaguti et al. (1999) pointed out that at least in one case (NGC 2110) this could be due to an incorrect modeling of a complex photoelectric absorber in the ASCA bandpass. To verify this hypothesis, we have extracted from the BeppoSAX archive the PDS spectra of the "flat" Seyfert 2s of the Turner et al. (1997) sample. In Fig. 3 we compare the Γ versus 2–10 keV (extrapolated) flux iso-χ^2 contours for NGC 1052 and the "flat" Seyfert 2s (the results for NGC 5252 are not shown, because the PDS detection is too weak). In all cases the intrinsic spectral index as measured by the PDS is significantly steeper than in ASCA. This suggests that the nature of the accretion flow in the nucleus of NGC 1052 is qualitatively different from that normally at work in bright nearby AGN.

The NGC 1052 high-energy spectrum is can be also well approximated by a thermal bremsstrahlung with $kT \simeq 150$ keV, in agreement with the expectations of the ADAF scenario. No estimate of the nuclear black hole mass is available for NGC 1052. If we use the bulge B magnitude (Ho et al. 1997) versus black hole mass relation of Magorrian et al. (1998), we obtain $M_{\rm BH} \sim 10^{8\pm1} M_\odot$. The bolometric luminosity of the ADAF component extrapolated from the BeppoSAX measurement is $\simeq 5 \times 10^{42}$ erg s^{-1}, suggesting an accretion rate $\dot{m} \sim 10^{-4\pm1}$. This value is significantly lower than the critical $\dot{m}$, below which the onset of the ADAF regime would occur (Narayan & Yi 1995).

Critical diagnostic tools for the existence of an ADAF are the radio-to-X-ray Spectral Energy Distribution (SED) and luminosity ratio (Di Matteo et al. 2000). In Fig. 4 we show the NGC 1052 radio/X-ray SED. The radio data points are taken from the NED archive. We observe a good qualitative agreement between the shape of the SED in NGC 1052 and in the "candidate-ADAF" elliptical galaxies of the Allen et al. (2000) sample. In Tab. 2 we compare the ratios between the powers at 6 keV and 5 GHz in these galaxies and in NGC 1052. In the latter this ratio is well within the (rather narrow) range observed in the former objects, confirming the qualitative similarity. For comparison, the value of this ratio is typically $\gtrsim 10^5$ in radio-quiet quasars (Elvis et al. 1994)

It is also interesting to compare the X-ray with the IR photometry of Becklin et al. (1982). Their 1.2μm flux in the innermost 2″ ($\simeq$300 pc) - 26 mJy - corresponds to a $L(1.25\ \mu m)/L(5\ keV)$ ratio of about 15. Such a high value is typical of Seyfert 2 galaxies (Mass-Hesse et al. 1995). The IR emission is therefore likely to be dominated by heated dust,

Source	$\log(P_{6\ \mathrm{keV}}/P_{5\ \mathrm{GHz}})$
NGC 1052	2.5
NGC 1399	2.0
NGC 4472	2.1
NGC 4486	2.8
NGC 4696	3.0
NGC 4649	2.7

Table 2. X-ray to radio power ratios in NGC 1052 and the candidate ADAF elliptical galaxies of Allen et al. (2000). The data for these objects are taken from Di Matteo et al. (2000)

totally masking the ADAF IR intrinsic emission and therefore preventing us from checking the presence of a wind in the ADAF scenario (Di Matteo et al. 2000).

The luminosity of the broad component of H_β is $\sim 2 \times 10^{41}$ erg s^{-1} (Ho et al. 1997; Barth et al. 1999). An ADAF cannot provide the corresponding amount of (mainly UV) ionizing photons. This points to a flow with a small sonic radius r_s, consistent with models where the viscosity parameter α is $\lesssim 10^{-2}$ ($r_\mathrm{s} \sim$ a few R_g; Narayan et al. 1997). Outside this radius the flow would smoothly connect to a standard thin accretion disk.

The BeppoSAX data alone cannot rule out the possibility that a substantial contribution to the hard X-ray emission comes from a nuclear relativistic jet. *Chandra* will have enough spatial resolution to image X-ray structures on scales as small as $\sim$100 pc. However, it is to be noted that the ROSAT HRI images of NGC 1052 unveiled only a soft X-ray extended emission on a much wider scale ($\sim$15 kpc) than that of the radio structures (G99), therefore probably due to the emission of diffuse intergalactic gas. The contribution of this component to the hard X-ray emission is most likely negligible.

Acknowledgements. The BeppoSAX satellite is a joint Italian-Dutch program.This research has made use of the NASA/IPAC Extragalactic Database (NED) which is operated by the Jet Propulsion Laboratory, California Institute of Technology, under contract with the National Aeronautics and Space Administration.

References

Allen S.W., Di Matteo T., Fabian A.C., 2000, MNRAS 311, 493
Antonucci R., Miller J., 1985, ApJ 297, 621
Barth A.J., Filippenko A.V., Moran E.C., 1999, ApJ 525, 673
Becklin E.E., Tokunaga A.T., Wynn-Williams C.G., 1982, ApJ 263, 624
Boella G., Chiappetti L., Conti G., et al., 1997, A&AS 122, 372
Cagnoni I. della Ceca R., Maccacaro T., 1998, ApJ 493, 54
Di Matteo T., Quataert E., Allen S.W., Narayan R., Fabian A.C., 2000, MNRAS 311, 507
Elvis M., Wilkes B.J., McDowell J.C., et al., 1994, ApJS 95, 1
Fabian A.C., Rees M.J., 1995, MNRAS, 277, L55
George I.M., Fabian A.C., 1991, MNRAS, 249, 352
Ghisellini G., Haardt F., Matt G., 1994, MNRAS, 267, 743
Guainazzi M., Antonelli L.A., 1999, MNRAS 304, L15 (G99)
Guainazzi M., Matteuzzi A., 1997, SDC-TR-014, available at `ftp://www.sdc.asi.it`
Guainazzi M., Perola G.C., Matt G., et al., 1999, A&A 346, 407
Heckman T.M., 1980, A&A 87, 152
Ho L.C., Filippenko A.V., Sargent W.L.W., 1997, ApJS 112, 315
Krolik J.H., Madau P., Zycki P.Y., 1994, ApJ 420, 57
Leahy D.A., Creighton J., 1993, MNRAS 263, 314
Magdziarz P., Zdziarski A.A., 1995, MNRAS 273, 837
Magorrian J., Tremaine S., Richstone D., et al., 1998, AJ, 115, 2285
Malaguti G., Bassani L., Cappi M., et al., 1999, A&A 342, L41
Mass-Hesse J.M., Rodríguez-Pascal P.M., Cordoba L.S.F., et al., 1995, A&A 298, 22
Matt G., 2000, Proceedings of the Conference "X-ray Astronomy '999", Malaguti G., Palumbo G. & White N. eds., (Gordon & Breach:Singapore), in press (astroph/0007050)
Matt G., Perola G.C., Piro L., Stella L., 1992, A&A 263, 453
Matt G., Brandt W.N., Fabian A.C., 1996, MNRAS 280, 823
Nandra K., George I.M., Mushotzky R.F., Turner T.J., Yaqoob T., 1997, ApJ 476, 70
Narayan R., Kato S., Honma F., 1997, ApJ 476, 49
Narayan R., Yi I., 1995, ApJ 452, 710
Netzer H., Turner T.J., 1997, ApJ 488, 694
Parmar A.N., Martin D.D.E., Bavdaz M., et al., 1997, A&AS 122, 309
Rees M.J., Phinney E.S., Begelman M.C., Blandford R.D., 1982, Nat 295, 17
Reeves J., Turner M., 2000, MNRAS, in press (astroph/0003080)
Reynolds C.S., 1997, MNRAS 286, 513
Turner T.J., George I.M., Nandra K., Mushotzky R.F., 1997, ApJS 113, 23
Weaver K.A., Wilson A.S., Henkel C., Braatz J.A., 1999, ApJ 520, 130
Wilkes B.J., Elvis M., 1987, ApJ 323, 243